Model dependence of charge-symmetry breaking in the neutron-proton interaction

M. Beyer
Paul Scherrer Institute, CH-5234 Villigen, Switzerland*

A. G. Williams
Institute for Nuclear Theory, Department of Physics, FM-15, University of Washington, Seattle, Washington 98195
(Received 18 April 1988)

The effects of charge-symmetry breaking of nuclear forces can be observed in neutron-proton elastic scattering as a difference between neutron and proton analyzing powers. A formalism has previously been developed and applied to compute these effects in terms of electromagnetic interactions, one-boson exchange potentials, the two-pion exchange potential, and possible quark effects. The results were found to be in agreement with the one existing measurement. Here we extend this work and study in detail how these charge-symmetry breaking predictions vary with the particular choice for the nucleon-nucleon force. We compare predictions for Reid soft-core, Paris, coordinate-space Bonn, and hybrid quark-meson potentials. We show in particular that charge-symmetry breaking measurements can place strong restrictions on models of the nucleon-nucleon interaction.

I. INTRODUCTION

Discussions of the significance of charge-symmetry breaking (CSB) have been given in a number of reviews.[1-3] Charge symmetry implies the invariance of a system under a transformation which reverses the sign of the third component of the isospin for all of its constituents (e.g., $p \rightarrow n$ and $n \rightarrow p$). Here we are concerned with the phenomenon of neutron (n)-proton (p) elastic scattering, which is of particular interest since the absence of Coulomb forces makes it possible to establish the existence of CSB unambiguously.

A recent TRIUMF experiment[4] has found evidence of CSB in this system by measuring a difference between neutron and proton analyzing powers in n-p elastic scattering at 477 MeV at the zero-crossing point of the analyzing power. Their nonzero result is a direct measurement of CSB, since it shows that the system is not invariant under the transformation $n \leftrightarrow p$. The difference in n and p analyzing powers is $\Delta A(\theta) \equiv A_n(\theta) - A_p(\theta)$, where $A_n(\theta)$ and $A_p(\theta)$ are the neutron and proton analyzing powers, respectively. Denoting the zero-crossing angle of the analyzing power in the center-of-mass (c.m.) system by $\theta_{\text{c.m.}}$ we define $\Delta A \equiv \Delta A(\theta_{\text{c.m.}})$. The quoted result at 477 MeV is $\Delta A = [37 \pm 17(\text{stat.}) \pm 8(\text{syst.})] \times 10^{-4}$, which is significant since CSB had not previously been established unambiguously.[1-3] An experiment at 350 MeV is planned at TRIUMF, while another at 188 MeV is proceeding at the Indiana University Cyclotron Laboratory (IUCF). Similar measurements at energies up to 800 MeV are possible at LAMPF.[5]

There have been a number of previous theoretical treatments of CSB in the n-p system.[1,6-8] Recent calculations[9,10] have found results in agreement with the one existing TRIUMF measurement. These calculations attempt to understand the nonzero result for ΔA in terms of electromagnetic (em) interactions, one-boson exchange potentials (OBEP), and the two-pion exchange potential (TPEP). Estimates of possible contributions from quark effects have also been made.[10] Our aim here is to extend the work of Refs. 9 and 10 by using the developed formalism to make a detailed comparison of CSB predictions from different theories. We consider in particular to what extent CSB measurements in the n-p system can be used to place constraints on theories of the nucleon-nucleon (N-N) force. The present work is complemented by recent calculations[11] of ΔA from a momentum-space OBEP. The reported results compared reasonably well with those of Refs. 9 and 10. An additional calculation[12] of the contribution to ΔA from the n-p mass difference using a relativistic formalism and a covariant representation of the N-N on-shell scattering matrix yielded smaller results. However, this relativistic approach contains no explicit potential and requires an arbitrary off-shell extrapolation of the T matrix. This treatment in effect uses a very soft pion form factor, which acts to reduce the dominant CSB contribution from one-pion exchange.

N-N forces can be divided into four classes[1] according to their isospin invariance, where only class III and IV potentials give rise to CSB. In the np system only class IV forces can contribute to CSB. The simplest such forces are

$$V^{\text{IV}} = (\tau_1 - \tau_2)_3 (\sigma_1 - \sigma_2) \cdot \mathbf{L} v(r) , \tag{1.1a}$$

$$V^{\text{IV}} = (\tau_1 \times \tau_2)_3 (\sigma_1 \times \sigma_2) \cdot \mathbf{L} w(r) , \tag{1.1b}$$

where $\mathbf{L}$ is the orbital angular momentum operator in the center-of-mass frame and $\mathbf{r} = \mathbf{r}_1 - \mathbf{r}_2$ is the internucleon separation. CSB in the np system requires mixing of

$T=0$ and $T=1$ states and, hence, also of $S=0$ and $S=1$ states. Then only $J=L$ states can contribute to CSB in n-p elastic scattering and hence to ΔA. The calculations are performed using the distorted-wave Born approximation (DWBA), where

$$V=V_{\rm CS}+V^{\rm IV} \tag{1.2}$$

and

$$\delta T_{fi}=\int d^3r\psi_f^{(-)\dagger}(\mathbf{r})V^{\rm IV}(\mathbf{r})\psi_i^{(+)}(\mathbf{r}) . \tag{1.3}$$

The initial and final distorted waves (ψ_i and ψ_f) are calculated from some charge-symmetric model of the N-N interaction ($V_{\rm CS}$).

In Sec. II we briefly review the formalism used in the calculations and the various class IV CSB potentials. A full discussion of these can be found elsewhere.[10] Only four significant contributions were found: (1) n-p mass difference in the one-pion exchange potential (OPEP), (2) one-photon exchange between the proton charge and the neutron anomalous magnetic moment, (3) mixed rho-omega exchange, and (4) n-p mass difference in one-rho exchange. The various choices of the (charge-symmetric) N-N interaction are discussed in Sec. III. We consider, in particular, the Reid soft-core (RSC),[13] Paris,[14] coordinate-space Bonn (OBEPR),[15] and Virginia-Mainz[16] (VMZ) hybrid quark-meson potentials. For the RSC and Paris potential cases typical values are chosen for the coupling constants and form factors in the evaluation of $V^{\rm IV}$. Since the Bonn (OBEPR) and VMZ potentials are OBEP models, we perform consistent calculations with the parameters of $V_{\rm CS}$ also used to calculate $V^{\rm IV}$. The numerical results are presented and the different models compared in Sec. IV.

II. CSB POTENTIALS

The elastic scattering of two spin-$\frac{1}{2}$ particles can always be specified in terms of six invariant amplitudes,[7,17] assuming only Lorentz invariance, parity conservation, and time-reversal invariance. These amplitudes $a,b,c,d,e,$ and f are complex functions of the total c.m. energy E_T and the c.m. scattering angle θ. The scattering matrix spin operator can be written as

$$\begin{aligned}\hat{M}=\tfrac{1}{2}[&(a+b)+(a-b)(\boldsymbol{\sigma}_1\cdot\mathbf{n})(\boldsymbol{\sigma}_2\cdot\mathbf{n})\\&+(c+d)(\boldsymbol{\sigma}_1\cdot\mathbf{m})(\boldsymbol{\sigma}_2\cdot\mathbf{m})\\&+(c-d)(\boldsymbol{\sigma}_1\cdot\mathbf{l})(\boldsymbol{\sigma}_2\cdot\mathbf{l})\\&+e(\boldsymbol{\sigma}_1+\boldsymbol{\sigma}_2)\cdot\mathbf{n}+f(\boldsymbol{\sigma}_1-\boldsymbol{\sigma}_2)\cdot\mathbf{n}] ,\end{aligned} \tag{2.1}$$

where $\mathbf{k}_i$ and $\mathbf{k}_f$ are the initial and final c.m. momenta for the scattered particle (particle 1) and where

$$\mathbf{l}\equiv\frac{\mathbf{k}_f+\mathbf{k}_i}{|\mathbf{k}_f+\mathbf{k}_i|},\quad \mathbf{m}\equiv\frac{\mathbf{k}_f-\mathbf{k}_i}{|\mathbf{k}_f-\mathbf{k}_i|},\quad \mathbf{n}\equiv\frac{\mathbf{k}_i\times\mathbf{k}_f}{|\mathbf{k}_i\times\mathbf{k}_f|} . \tag{2.2}$$

It is straightforward to show[10] that the difference in n-p analyzing powers is given by

$$\Delta A(\theta)\equiv A_n(\theta)-A_p(\theta)=2\,{\rm Re}(b^*f)/\sigma_0 , \tag{2.3}$$

where σ_0 is the unpolarized cross section

$$\begin{aligned}\sigma_0&\equiv\left[\frac{d\sigma}{d\Omega}\right]_{\rm unpol}\\&=\tfrac{1}{4}{\rm Tr}(\hat{M}\hat{M}^\dagger)=\tfrac{1}{2}(|a|^2+|b|^2+|c|^2\\&\quad+|d|^2+|e|^2+|f|^2) .\end{aligned} \tag{2.4}$$

As was already discussed, CSB in n-p scattering requires spin singlet-triplet mixing and, hence, requires $f(k,\theta)\neq0$ in Eq. (2.1), where $k\equiv|\mathbf{k}_i|=|\mathbf{k}_f|$.

The bar phase-shift L-S representation of the N-N scattering matrix[18] can be extended to include a new parameter $\bar{\gamma}_J$ (the spin singlet-triplet mixing angle). This representation can then be related to the six amplitudes of Eq. (2.1) and, in particular, it can be shown[7] that

$$\begin{aligned}f(k,\theta)=\frac{i}{2k}\sum_{J=1}^{\infty}&(2J+1)\sin(2\bar{\gamma}_J)\\&\times\exp(i\bar{\delta}_J+i\bar{\delta}_{JJ})d^J_{10}(\theta) ,\end{aligned} \tag{2.5}$$

where the d^J_{10} are the Wigner functions and $\bar{\delta}_J$ and $\bar{\delta}_{JJ}$ are the singlet and uncoupled triplet bar phase shifts, respectively. Use of the DWBA and using $\sin(2\bar{\gamma}_J)\simeq2\bar{\gamma}_J$ (since $\bar{\gamma}_J$ is very small) allows $V^{\rm IV}$ to be related to $f(k,\theta)$ and hence to $\bar{\gamma}_J$. This gives

$$\bar{\gamma}_J=-2E_Tk\sqrt{J(J+1)}\int_0^\infty dr\,r^2R_J(r)g(r)R_{JJ}(r) , \tag{2.6}$$

where $E_T\equiv$(total) c.m. energy $\equiv2E$ with E the energy per nucleon in the c.m. frame and where

$$g(r)\equiv v(r)\text{ and }(-1)^Jw(r) \tag{2.7}$$

for Eqs. (1.1a) and (1.1b), respectively. The distorting effects of the strong interaction are included through the radial wave functions $R_J(r)$ and $R_{JJ}(r)$, both of which are normalized such that

$$R(r)\xrightarrow[r\to\infty]{}\sin(kr-\tfrac{1}{2}J\pi+\bar{\delta})/kr , \tag{2.8}$$

where $\bar{\delta}\equiv\bar{\delta}_J$ and $\bar{\delta}_{JJ}$ for $R_J(r)$ and $R_{JJ}(r)$, respectively. The radial wave functions $R(r)$ are calculated for each of the N-N interactions (i.e., for each $V_{\rm CS}$) to be discussed in Sec. III. The charge-symmetric bar phase shifts (i.e., excluding $\bar{\gamma}_J$) are taken from the phase-shift analysis of Arndt *et al.*[19] We do this in order that we obtain the correct analyzing power zero-crossing angle for the different theories. In this sense we are not performing a completely consistent calculation[11] for each theory. However, our objective is to obtain the most reliable estimates possible for ΔA and to meaningfully compare ΔA predictions from the different theories.

The CSB contributions considered in Refs. 9 and 10 are shown in Fig. 1, with the exception of those arising from quark effects. We neglect the TPEP and quark contributions since they were found to be very small. In evaluating contributions from these one-boson exchange

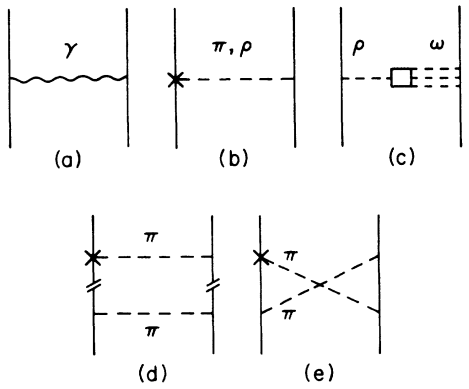

FIG. 1. The charge-symmetry breaking processes considered (with the exception of quark effects). Shown are (a) one-photon, (b) one-pion or one-rho, (c) mixed rho-omega, and (d) uncrossed and (e) crossed two-pion exchanges. The crosses indicate the CSB vertex function arising from the neutron-proton mass difference. The cross hatching refers to the usual subtraction procedure in (d). Only (a), (b), and (c) have been found to have significant effects.

diagrams the form factors applied to *each vertex* were[15] ($\mathbf{q}\equiv\mathbf{k}_f-\mathbf{k}_i$)

$$F_\alpha(\mathbf{q}^2)\equiv\left[\frac{\Lambda_\alpha^2-m_\alpha^2}{\Lambda_\alpha^2+\mathbf{q}^2}\right]^{n_\alpha}, \tag{2.9}$$

where $\alpha=\gamma$, π, ρ, and ω. The exception is the VMZ potential[16] which uses Gaussian form factors derived from the constituent quark model. The form factors are not explicitly included in the following equations, but are to be understood.

The one-photon exchange CSB contribution has the form of Eq. (1.1a):

$$v_\gamma(r)=-\left[\frac{e^2}{4\pi}\right]\frac{\kappa_n}{4M^2}\left[\frac{M}{E}\right]\frac{1}{r}\frac{d}{dr}\left[\frac{1}{r}\right], \tag{2.10}$$

where $\kappa_n=-1.91$ is the anomalous magnetic moment of the neutron ($e^2/4\pi=\frac{1}{137}$ is the fine-structure constant, and $M=938.93$ MeV is the nucleon mass. The γNN vertex form factor used here had $n_\gamma=2$ and $\Lambda_\gamma=842.6$ MeV, which is the conventional dipole fit to the experimental[20] proton form factor (c.f. Ref. 10). The (M/E) factor is a relativistic correction. The infinite range of the em interaction causes large J contributions to be important. However, since form factors and nuclear distortion become negligible for $J\gtrsim 5$ an excellent analytic estimate can be made for the sum of all higher partial waves.[7,10]

The *n-p* mass difference gives rise to a class IV CSB potential in both charged one-pion and charged one-rho exchange diagrams. The OPEP contribution has the form of Eq. (1.1b):

$$w_\pi(r)=-\left[\frac{g_\pi^2}{4\pi}\right]\frac{1}{2M^2}\left[\frac{M}{E}\right]^3\left[\frac{M_n-M_p}{2M}\right]\frac{1}{r}\frac{d}{dr}\left[\frac{1}{r}e^{-m_\pi r}\right], \tag{2.11}$$

where $(M_n-M_p)=1.293$ MeV is the *n-p* mass difference and $(M/E)^3$ is a relativistic correction. The exact choice of $(g_\pi^2/4\pi)$, m_π, and form factor depend on the potential being considered and will be discussed in Sec. III. The one-rho exchange contribution has pieces of the form of both Eqs. (1.1a) and (1.1b):

$$v_\rho(r)=-\left[\frac{g_\rho^2}{4\pi}\right]\frac{1}{4M^2}\left[\frac{M}{E}\right]^3\left[\frac{M_n-M_p}{2M}\right]\frac{1}{r}\frac{d}{dr}\left[\frac{1}{r}e^{-m_\rho r}\right] \tag{2.12a}$$

$$w_\rho(r)=-\left[\frac{g_\rho^2}{4\pi}\right]\left[1+\frac{E+3M}{2M}\frac{f_\rho}{g_\rho}+\frac{E+M}{2M}\left[\frac{f_\rho}{g_\rho}\right]^2\right]\frac{1}{2M^2}\left[\frac{M}{E}\right]^3\left[\frac{M_n-M_p}{2M}\right]\frac{1}{r}\frac{d}{dr}\left[\frac{1}{r}e^{-m_\rho r}\right], \tag{2.12b}$$

where again a relativistic correction has been included and $(g_\rho^2/4\pi)$, (f_ρ/g_ρ), m_ρ, and Λ_ρ will be chosen later.

Another contribution comes from mixed rho-omega exchange. Since the rho and omega mesons are isovector and isoscalar, respectively, this obviously allows $T=0$ and $T=1$ mixing. The ρ-ω mixing matrix element has been extracted from experimental data by a number of groups[1,21] with values for $\langle\omega\,|\,H\,|\,\rho^0\rangle$ ranging from -3400 to -6000 MeV^2. A recent treatment[22] drawing on new data argues for a value of -4520 MeV^2. We will follow Ref. 10 here and use the conservative value[23] for ease of comparison:

$$\langle\omega\,|\,H\,|\,\rho^0\rangle=-3400\ \text{MeV}^2\ . \tag{2.13}$$

The ρ-ω mixing contribution to ΔA is essentially proportional to (2.13). The uncertainty in the ρ and ω coupling constants leads to an uncertainty in this effect of *at least* 30%. The resulting class IV potential has the form of Eq. (1.1a):

$$v_{\rho\omega}(r)=-\frac{f_\rho g_\omega}{4\pi}\frac{1}{2M^2}\frac{\langle\omega\,|\,H\,|\,\rho^0\rangle}{m_\omega^2-m_\rho^2}\times\frac{1}{r}\frac{d}{dr}\left[\frac{e^{-m_\rho r}-e^{-m_\omega r}}{r}\right]. \tag{2.14}$$

No relativistic correction is included, and so for consistency $E_T\to 2M$ in Eq. (2.6) for this contribution. As for the π and ρ parameters, $(g_\omega^2/4\pi)$, (f_ω/g_ω), m_ω, and Λ_ω will be fixed according to the particular *N-N* potential being considered.

III. *N-N* POTENTIALS

We now discuss the charge-symmetry part of the *N-N* interaction. We have chosen different distorting potentials to investigate the model dependence of ΔA. As stated in the Introduction we have chosen for this purpose the RSC,[13] Paris,[14] Bonn[15] (OBEPR), and VMZ (Ref. 16) potentials. These models differ strongly in their treatment of the short-range part of the *N-N* interaction.

Some of these models have been discussed previously in this context. Extensive calculations with the RSC potential can be found elsewhere.[10] A calculation using the Paris potential has been reported,[8] but did not include sufficient partial waves for the em contribution. A momentum-space version of the Bonn potential has also been used to evaluate ΔA.[11] Calculations in the plane-wave Born approximation have been made and show the importance of including the effects of distortion.[10] However, to date no systematic investigation of the model dependence of these predictions has been carried out.

The RSC potential uses Yukawa potentials to parameterize the *N-N* force. Only the long-range part can be identified with an existing meson, i.e., the pion. Medium- and short-range parts are purely phenomenological. For partial waves with $L>2$ the potential is set to zero.

The original version of the Paris potential was based on dispersion theory and introduced a phenomenological, energy-dependent potential for $r<0.8$ fm to treat the short-range *N-N* interaction. In our calculations the coordinate space version[14] was used, which is a parametrization in terms of a regulated sum of Yukawa-type interactions.

The Bonn potential used here is the coordinate-space version (OBEPR) with the parameters of Table 14 in Ref. 15. It is a nonrelativistic one-boson exchange model with parameters chosen to give the best fit to empirical data. The experimental elastic phase shifts are reproduced reasonably well for $E_{\rm lab}<350$ MeV, except for the $^1P_1$ phase shift. The short-range repulsion of the *N-N* force arises from an ω exchange, with a large ωNN coupling constant, $g^2_{\omega NN}/4\pi=20$. The Bonn form factors have the form given in Eq. (2.9).

The VMZ potential is a hybrid model that combines quark degrees of freedom and quantum chromodynamics (QCD) symmetries with the successful OBEP description of the *N-N* force. The quark degrees of freedom in the short-range part of the potential are treated via an optical potential with discrete energy levels for the six-quark core. This model was motivated by the compound quark bag model of Ref. 24. We have considered two different versions, where the six-quark core radius is either $b=1$ fm or $b=1.2$ fm. The medium- and long-range parts are described by a meson exchange model with coupling constants fixed by QCD symmetries. In this model a constituent quark model with relativistic corrections was used as the basis to determine coupling constants and vertex form factors. The boson masses and coupling constants are given in Table 2 of Ref. 16 (1987). The vertex form factors of Eq. (2.9) for simple, one-boson exchange lead to the momentum-space replacement

$$\frac{1}{(\mathbf{q}^2+m_\alpha^2)}\rightarrow\frac{1}{(\mathbf{q}^2+m_\alpha^2)}\left[\frac{\Lambda_\alpha^2-m_\alpha^2}{\Lambda_\alpha^2+\mathbf{q}_\alpha^2}\right]^{2n_\alpha}. \tag{3.1}$$

The vertex form factors for the VMZ potential give rise to a Gaussian function

$$\frac{1}{(\mathbf{q}^2+m_\alpha^2)}\rightarrow\frac{1}{(\mathbf{q}^2+m_\alpha^2)}\exp(-\mathbf{q}^2/3\alpha_0^2), \tag{3.2}$$

where $\alpha_0^2=2.8$ fm^{-2} is the spring constant of the harmonic oscillator potential. The form factors are identical for each meson vertex (i.e., π, ρ, ω, etc.) in the VMZ generated CSB potentials. This form factor gives rise to the coordinate-space replacement[16] in Eqs. (2.11), (2.12), and (2.14):

$$\frac{1}{r}\exp(-m_\alpha r)\rightarrow m_\alpha\exp(x_0^2)/2x\left[e^{-x}\,\mathrm{erfc}\left[x_0-\frac{x}{2x_0}\right]-(x\rightarrow -x)\right], \tag{3.3}$$

where $x\equiv m_\alpha r$, $x_0\equiv(m_\alpha/\alpha_0\sqrt{3})$, $\mathrm{erfc}(z)\equiv 1-\mathrm{erf}(z)$, and erf is the usual error function. In the limit $\alpha_0\rightarrow\infty$ the point nucleon limit is recovered [i.e., rhs $\rightarrow$ lhs of Eq. (3.3)]. For the γNN vertex in the VMZ model it is also consistent to use the usual dipole form factor, since the underlying constituent quark model reproduces the data to within 10% if relativistic corrections are included.[25]

In the VMZ model for $r<b$ the *N-N* system has both a nonhadronic six-quark component and the usual two-hadron component. The class IV CSB potentials given in Sec. II are applicable only for the two-hadron component. In Ref. 10 an estimate of the class IV CSB contribution from a six-quark core was found to be negligible. The quark spatial wave functions were in the completely symmetric,[6] which has only a very small two-nucleon component and so is essentially orthogonal to the two-hadron component. Thus, the only significant contribution to a class IV potential is the two-nucleon contribution given by the equations in Sec. II.

While it is clear what masses, coupling constants, and form factors to use in the class IV potentials for the Bonn (OBEPR) and VMZ potentials, the best we can do for the RSC and Paris potentials is to choose typical values from low-energy analyses.[26,27] For these two potentials we have used exactly the same parameters as Ref. 10 (except for the choice of the γNN vertex form factor). The various parameters relevant to the class IV potentials are summarized in Table I.

All of the potentials give a reasonable description of the deuteron properties and the elastic scattering data for $E_{\rm lab}\lesssim 350$ MeV.

IV. NUMERICAL RESULTS

The results of our calculations of ΔA are shown in Table II for four energies of interest. The one experimental result from TRIUMF (Ref. 4) at 477 MeV is also shown. We illustrate the angular dependence of the contributions to the analyzing power difference in Figs. 2(a)–(d) for $E_{\rm lab}=477$ MeV. The differences between the

TABLE I. The meson parameters used in the class IV potentials of Sec. II. All masses are in MeV and $n_\alpha = 1$ for $\alpha = \pi, \rho, \omega$.

	RSC Paris	Bonn (OBEPR)	VMZ $b = 1$ fm	VMZ $b = 1.2$ fm
$g_\pi^2/4\pi$	14.4	14.9	13.4	14.0
m_π	139.57	138.03	138.5	138.5
Λ_π	1300	1300		
$g_\rho^2/4\pi$	0.55	0.95	1.05	1.10
f_ρ/g_ρ	6.1	6.1	1.53	1.53
m_ρ	770	769	763	763
Λ_ρ	1400	1300		
$g_\omega^2/4\pi$	8.1	20	9.44	9.85
m_ω	783	782.6	782.3	782.3
Λ_ω	1500	1500		

predictions of the four N-N potentials in this figure is typical of what was also found at the other energies. All of the predictions for ΔA at 477 MeV lie within one standard deviation of the experimental result, with the obvious exception of the Bonn (OBEPR) potential.

While we used relativistic kinematics throughout, the Schrödinger equation was used for calculating the distorted wave functions. This is adequate for the lower energies ($E_{\rm lab} \leq 350$ MeV) where the potentials have been fitted to the experimental phase shifts, but there is some small uncertainty in the calculation at 477 MeV, which can be expected to worsen at 600 MeV. In the Schrödinger equations for the VMZ potential, a relativistic correction was included.[16] These distorted wave functions are then used in Eq. (2.6) to calculate the mixing angles $\bar{\gamma}_J$ for each of the potentials.

In order to obtain the correct analyzing power zero-crossing angle and to make a meaningful comparison of the different N-N potentials, the charge-symmetric phase shifts are taken from the phase shift analysis of Ref. 19. We linearly interpolate these phenomenological phase shifts to the energies of interest and use them together with the calculated mixing angles $\bar{\gamma}_J$ to calculate $\Delta A(\theta)$ and ΔA. In particular for 188 and 350 MeV the 1983 n-p energy-dependent phase shifts were used, while for the higher energies of 477 and 600 MeV the more recent 1987 n-p single energy analysis phase shifts were taken. The recent analyses include high-energy data.

At 477 MeV there are already inelasticities in the $^1D_2$ and $^3P_1$ channels and no account is taken of these in the calculations. However, previous estimates[10] of their importance have been made and it was argued that their influence is relatively small. Future work should attempt to explicitly include pionic degrees of freedom, particularly at higher energies.

For the π, ρ, and ρ-ω contributions we keep partial

TABLE II. Comparison of the various model predictions of $\Delta A(\times 10^4)$ at four energies of interest and the one experimental result at 477 MeV. Shown are the laboratory kinetic energy $E_{\rm lab}$, the c.m. angle (in deg) at which the analyzing power goes to zero $\theta_{\rm c.m.}$, and the separate contributions from π, γ, ρ-ω, and ρ exchanges. The different nucleon-nucleon potentials used are the Reid soft-core (RSC), Paris, coordinate-space Bonn (OBEPR), and Virginia-Mainz (VMZ) potentials. The VMZ potential is a hybrid quark-meson potential and the two versions considered here have a six-quark core radius of $b = 1$ fm and 1.2 fm, respectively.

$E_{\rm lab}$ (MeV)	$\theta_{\rm c.m.}$ (deg)	Potential	π	γ	$\rho\omega$	ρ	Total	Expt.
		RSC	7	8	5	1	21	
		Paris	11	10	7	2	30	
188	96	Bonn (OBEPR)	16	12	22	5	55	
		VMZ $b = 1$	8	9	4	1	22	
		VMZ $b = 1.2$	9	10	5	1	25	
		RSC	42	4	−3	6	49	
		Paris	47	8	3	8	66	
350	72	Bonn (OBEPR)	64	13	32	21	130	
		VMZ $b = 1$	36	6	−1	4	45	
		VMZ $b = 1.2$	41	9	2	4	56	
		RSC	43	7	−6	8	52	
		Paris	46	12	2	10	70	
477	70	Bonn (OBEPR)	67	16	38	27	148	37±17±8
		VMZ $b = 1$	35	7	−3	4	43	
		VMZ $b = 1.2$	41	12	2	5	60	
		RSC	34	13	−5	9	51	
		Paris	33	18	4	9	64	
600	70	Bonn (OBEPR)	54	22	42	26	144	
		VMZ $b = 1$	26	13	−1	4	42	
		VMZ $b = 1.2$	31	17	4	5	57	

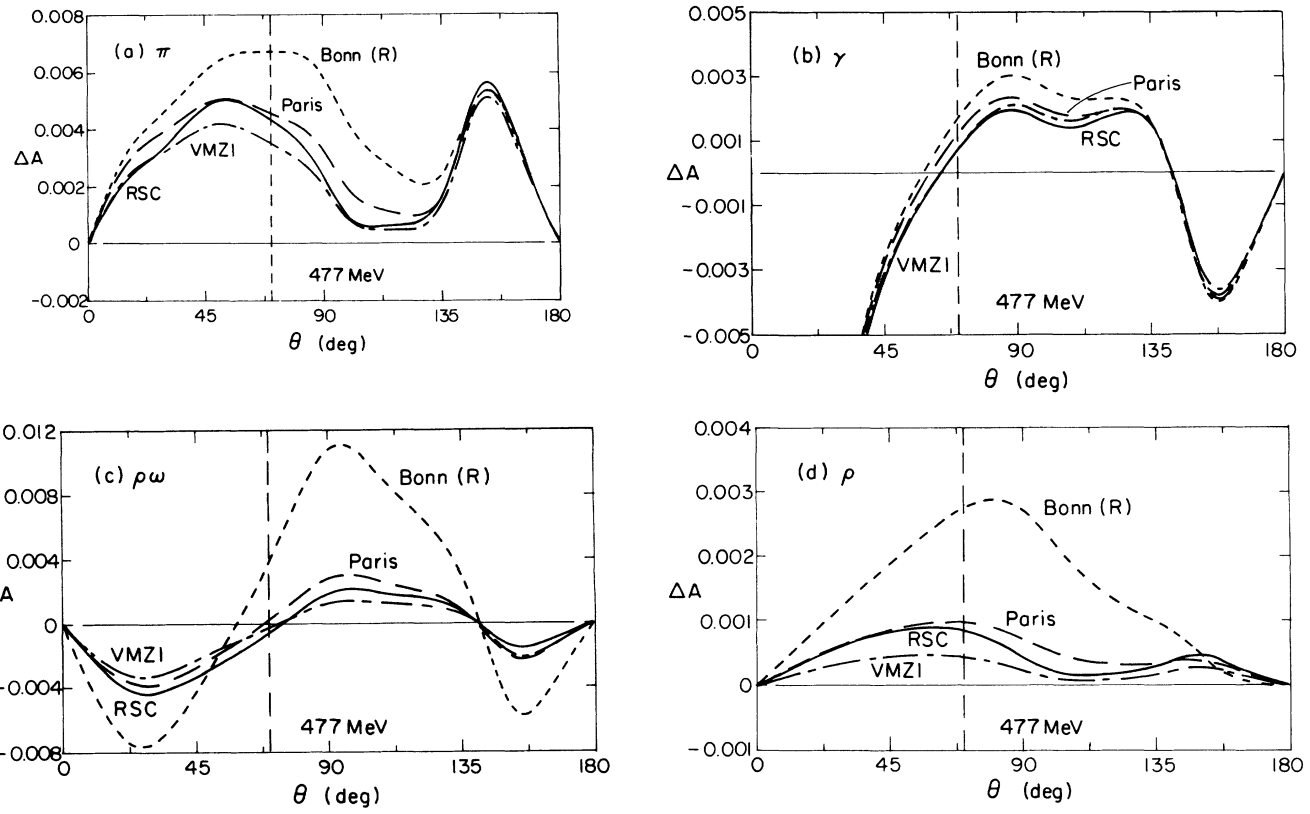

FIG. 2. The contributions to $\Delta A(\theta)$ at 477 MeV as a function of the c.m. scattering angle θ. Shown separately are the (a) pion, (b) em, (c) rho-omega, and (d) rho contributions. Each figure compares the results for the Reid soft-core (RSC) (—), Paris (— — —), coordinate-space Bonn (OBEPR) (- - - -), and $b=1$ Virginia-Mainz (VMZ1) (—·—·—·) potentials. The vertical dashed line indicates the analyzing power zero-crossing angle $\theta_{\text{c.m.}}=70°$.

waves up to $J=8$. As explained in Sec. II for the γ contribution we use analytic results for $J>5$. Since this em contribution is long range the numerical integration was performed out to $r=100$ fm in Eq. (2.6) to ensure accuracy. There are only two minor differences between the RSC calculations of Ref. 10 and those reported here. The dipole form factor for the γNN vertex is used here and we keep up to $J=8$ for π, ρ, and ρ-ω. A comparison of these two sets of RSC results shows that they give essentially identical predictions.

The RSC and Paris cases differ *only* in the distorted radial wave functions R_J and R_{JJ} in Eq. (2.6), since all other parameters were chosen to be the same. This is true for the γ contribution for *all* of the potentials, since the long-range one-photon exchange is well understood. To a lesser extent the same applies to the π contribution (see Table I). A comparison of Figs. 2(a) and 2(b) shows that all one-photon exchange contributions compare well, whereas significant differences begin to appear in the OPEP contribution. This results because the em interaction is long range and has significant contributions from high partial waves where the differences between the potentials are becoming very small. Conversely the π contribution is dominated by the low partial waves, which are very sensitive to the detailed short-range behavior of the N-N potential models. Hence, we see that shorter-range CSB contributions have increased sensitivity to the radial distortion of the low partial waves, which is exactly what we would expect.

For the ρ and ρ-ω contributions another source of significant differences between the potentials is in the ρ and ω coupling constants, masses, and form factors. For example, we find from Eqs. (2.6)–(2.14) that $\bar{\gamma}_J$ (for ρ) $\propto g_\rho^2$ and $\bar{\gamma}_J$ (for ρ-ω) $\propto f_\rho g_\omega$, which enhances the Bonn (OBEPR) results over those of RSC by $0.95/0.55 \simeq 1.7$ (for ρ) and $\simeq 2.1$ (for ρ-ω). From the $f_\rho g_\omega$ factor the ρ-ω contribution from the VMZ potentials will be suppressed with respect to RSC by a factor of $\simeq 2.7$. Since Eq. (2.12b) is expected to dominate the ρ contribution due to the extra $(-1)^J$ factor in Eq. (2.7) (see discussion in Ref. 9) we have the approximate relation

$$\bar{\gamma}_J \text{ (for } \rho) \propto g_\rho^2 \left[1+2\frac{f_\rho}{g_\rho} + \left[\frac{f_\rho}{g_\rho} \right]^2 \right],$$

which implies a suppression factor of $\simeq 4$ for VMZ with respect to RSC. Different distortions, masses, and form factors will, of course, cause deviations from these simple relations. It is clear from an examination of Figs. 2(c) and 2(d) that for the ρ and ρ-ω contributions the above

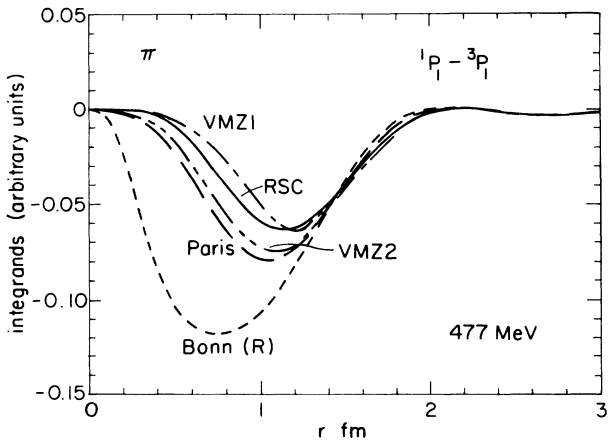

FIG. 3. The integrands for the π contribution to $\bar{\gamma}_1$ at 477 MeV after scaling out the coupling constant $(g_\pi^2/4\pi)$ (form factors are included), i.e., see Eq. (2.6). The Bonn (OBEPR) integrand has a peak almost twice as large as the others and it occurs at $\simeq 0.7$ fm than $\simeq 1-1.2$ fm.

arguments do explain the qualitative differences between the predictions of the different *N-N* potentials.

The Bonn (OBEPR) potential clearly stands out from the others and gives a prediction which is three times larger than the experimental result. This is partly due to the large ρ and ω coupling constants and partly due to differences in distortion for the low partial waves. We found in particular that $\bar{\gamma}_1$ was increased significantly by the radial distortion in the Bonn (OBEPR) potential compared to the others. This is illustrated in Fig. 3, where the integrands for the π contribution to $\bar{\gamma}_1$ at 477 MeV are compared after scaling out g_π^2 (form factors are included). This indicates a difference in the *P* waves, which may be related to the relatively poor fit to the $^1P_1$ phase shift. It seems reasonable to conclude that the Bonn (OBEPR) potential is not giving a good description of the short-range *N-N* interaction. This may be a result of the rather large ωNN coupling constant which provides a strong short-range repulsion in the *N-N* system.

For clarity only the VMZ potential with $b=1$ fm is shown in Fig. 2, although the $b=1.2$ fm results are somewhat similar. The $b=1$ fm case gives a slightly better fit to the deuteron magnetic form factor and the $^3P_1$ phase shifts. As is evident from Table II both versions give comparable results for ΔA at all energies and at 477 MeV both are in agreement with the experimental result.

There is, of course, some dependence on the choice of charge-symmetric phase shifts in the calculation of $\Delta A(\theta)$. When the 1987 phase shifts of Ref. 19 at 477 MeV are replaced with the 1983 phase shifts very little change results.[10] However, if a *fully* consistent calculation is performed (i.e., using the charge-symmetric phase shifts from the *N-N* potential being considered), more significant changes may result. This is particularly true if the predicted phase shifts do not correctly reproduce the correct zero-crossing angle for the analyzing power. This question has been discussed briefly for the case of a momentum-space OBEP in Ref. 11.

V. CONCLUSIONS

We have applied a previously developed formalism[10] for studying charge-symmetry breaking in *n-p* elastic scattering in terms of γ, π, ρ, and mixed ρ-ω exchanges (the contributions from two-pion and quark effects are negligible). Our aim was to examine the model dependence of the charge-symmetry breaking predictions. The charge-symmetric *N-N* potential models considered were the Reid soft-core, Paris, coordinate-space Bonn, and Virginia-Mainz potentials. These models differ principally in their treatment of the short-range part of the *N-N* interaction. Where possible the same parameters used in the charge-symmetric *N-N* potential were also used to evaluate the charge-symmetry breaking potentials.

We found reasonable agreement with the one existing experimental result at 477 MeV, with the exception of the coordinate-space Bonn potential. We have argued that the long-range π and γ contributions are relatively well understood and that most of the variation arises from the uncertainties in the short-range behavior of the charge-symmetric potentials, and the ρ and ω coupling constants. We concluded that the coordinate-space Bonn potential is not providing an adequate description of the short-range *N-N* interaction. Without additional experimental data it is not possible to make similar comments about the remaining potentials. It is worth noting that comparisons can also be made in one-boson exchange models of the parity violating *N-N* force.[28]

We have shown that charge-symmetry breaking can be a useful probe of short-distance behavior in the *N-N* system. A number of theoretical refinements are desirable, but it is essential to have more data. We are looking forward to results from IUCF at 188 MeV and TRIUMF at 350 MeV.

ACKNOWLEDGMENTS

We thank L. D. Knutson for providing his program to compute ΔA from the generalized bar phase shifts. One of us (A.G.W.) gratefully acknowledges a number of helpful discussions with G. A. Miller. This work was supported in part by the U.S. Department of Energy and the Deutsche Forschungsgemeinschaft Grant BE 1092/1-1.

*Formerly Swiss Institute for Nuclear Research (SIN).

[1]E. M. Henley and G. A. Miller, in *Mesons in Nuclei*, edited by M. Rho and D. H. Wilkinson (North-Holland, Amsterdam, 1979), p. 405.

[2]W. T. H. van Oers, Nucl. Phys. **A416**, 267c (1984).

[3]S. E. Vigdor, Invited Talk at the International Conference on Current Problems in Nuclear Physics, Crete, 1985 (unpublished); S. E. Vigdor *et al.*, in *Polarization Phenomena in Nu-*

clear Physics—1980 (Fifth International Symposium, Santa Fe), Proceedings of the Fifth International Symposium on Polarization Phenomena in Nuclear Physics, AIP Conf. Proc. No. 69, edited by G. G. Ohlsen *et al.* (AIP, New York, 1981), Vol. 2, p. 1455.

[4]R. Abegg *et al.,* Phys. Rev. Lett. **56**, 2571 (1986).

[5]J. C. Hiebert and L. C. Northcliffe, private communication.

[6]C.-Y. Cheung, E. M. Henley, and G. A. Miller, Nucl. Phys. **A305**, 342 (1978); **A348**, 365 (1980); C.-Y. Cheung, Ph.D. thesis, University of Washington, 1979 (unpublished).

[7]A. Gersten, Phys. Rev. C **24**, 2174 (1981); **18**, 2252 (1978).

[8]L. Ge and J. P. Svenne, Phys. Rev. C **33**, 417 (1986); **34**, 756 (1987). This work included a sign error in the OPEP contribution to $\bar{\gamma}_J$ which originally appeared in Ref. 6. The values of $\bar{\gamma}_J$ shown in this reference are actually 4π multiplied by $\bar{\gamma}_J$ (rad).

[9]G. A. Miller, A. W. Thomas, and A. G. Williams, Phys. Rev. Lett. **56**, 2567 (1986).

[10]A. G. Williams, A. W. Thomas, and G. A. Miller, Phys. Rev. C **36**, 1956 (1987).

[11]B. Holzenkamp, K. Holinde, and A. W. Thomas, Phys. Lett. **195B**, 121 (1987).

[12]M. J. Iqbal, J. Thaler, and R. M. Woloshyn, Phys. Rev. C **36**, 2442 (1987).

[13]R. V. Reid, Ann. Phys. (N.Y.) **50**, 411 (1968).

[14]M. Lacombe *et al.,* Phys. Rev. C **21**, 861 (1980); R. Vinh Mau, Nucl. Phys. **A374**, 3c (1982).

[15]R. Machleidt, K. Holinde, and Ch. Elster, Phys. Rep. **149**, 1 (1987), and references therein.

[16]M. Beyer and H. J. Weber, Phys. Rev. C **35**, 14 (1987); Phys. Lett. **146B**, 383 (1984); M. Bozoian and H. J. Weber, Phys. Rev. C **28**, 811 (1983).

[17]J. Bystricky, F. Lehar, and P. Winternitz, J. Phys. (Paris) **45**, 207 (1984).

[18]H. P. Stapp, T. J. Ypsilantis, and N. Metropolis, Phys. Rev. **105**, 302 (1957).

[19]R. A. Arndt *et al.,* Phys. Rev. C **15**, 1002 (1977); Phys. Rev. D **28**, 97 (1983); **35**, 128 (1987).

[20]G. G. Simon *et al.,* Nucl. Phys. **A333**, (1980).

[21]P. C. McNamee, M. D. Scadron, and S. A. Coon, Nucl. Phys. **A249**, 483 (1975); S. A. Coon, M. D. Scadron, and P. C. McNamee, *ibid.* **A287**, 381 (1977); J. L. Friar and B. F. Gibson, Phys. Rev. C **17**, 1752 (1978).

[22]S. A. Coon and R. C. Barrett, Phys. Rev. C **36**, 2189 (1987).

[23]Note that a negative sign was inadvertently omitted from this matrix element in Ref. 10, although it was included in all calculations.

[24]Yu. A. Simonov, Phys. Lett. **107B**, 1 (1981); Nucl. Phys. **A416**, 109c (1984); Yad. Fiz. **38**, 1542 (1983) [Sov. J. Nucl. Phys. **38**, 939 (1983)].

[25]M. Beyer and S. K. Sinh, Phys. Lett. **160B**, 26 (1985).

[26]O. Dumbrajs *et al.,* Nucl. Phys. **B216**, 277 (1983).

[27]W. Grein and P. Kroll, Nucl. Phys. **A338**, 332 (1980).

[28]D. E. Driscoll and G. A. Miller, private communication.